Histone mRNA is subject to 3' uridylation and re-adenylation in Aspergillus nidulans

Mossanen-Parsi, A., Parisi, D., Browne-Marke, N., Bharudin, I., Connell, S. R., Mayans, O., Fucini, P., Morozov, I. & Caddick, M. X.

RESEARCH ARTICLE

WILEY

Histone mRNA is subject to 3′ uridylation and re-adenylation in *Aspergillus nidulans*

Amir Mossanen-Parsi[1] | **Daniele Parisi[1,2]** | **Natasha Browne-Marke[3]** | **Izwan Bharudin[1]** | **Sean R. Connell[2,4]** | **Olga Mayans[1]** | **Paola Fucini[2,4]** | **Igor Y. Morozov[1,3]** | **Mark X. Caddick** [iD] **[1]**

[1]Institute of Systems, Molecular and Integrative Biology, The University of Liverpool, Liverpool, UK

[2]Center for Cooperative Research in Biosciences (CIC bioGUNE), Basque Research and Technology Alliance (BRTA), Derio, Spain

[3]Centre for Sport, Exercise and Life Sciences, Coventry University, Coventry, UK

[4]IKERBASQUE, Basque Foundation for Science, Bilbao, Spain

Correspondence
Paola Fucini, Center for Cooperative Research in Biosciences (CIC bioGUNE), Basque Research and Technology Alliance (BRTA), Bizkaia Technology Park, Building 801A, 48160 Derio, Spain.
Email: pfucini@cicbiogune.es

Igor Y. Morozov, Centre for Sport, Excercise and Life Sciences, Coventry University, Coventry, UK CV1 2DS
Email: ab6069@coventry.ac.uk (I. Y. M.)

Mark X. Caddick, The University of Liverpool, Institute of Systems, Molecular and Integrative Biology, Biosciences Building, Crown Street, Liverpool, L69 7ZB, UK. and caddick@liverpool.ac.uk (M. X. C.)

Present address
Natasha Browne-Marke, Division of Biomedical Science, University of Warwick, Coventry, UK
Izwan Bharudin, Department of Biological Sciences and Biotechnology, Faculty of Science and Technology, Universiti Kebangsaan Malaysia, Bangi, Malaysia Olga Mayans, Department of Biology, University of Konstanz, Konstanz, Germany

Abstract

The role of post-transcriptional RNA modification is of growing interest. One example is the addition of non-templated uridine residues to the 3′ end of transcripts. In mammalian systems, uridylation is integral to cell cycle control of histone mRNA levels. This regulatory mechanism is dependent on the nonsense-mediated decay (NMD) component, Upf1, which promotes histone mRNA uridylation and degradation in response to the arrest of DNA synthesis. We have identified a similar system in *Aspergillus nidulans*, where Upf1 is required for the regulation of histone mRNA levels. However, other NMD components are also implicated, distinguishing it from the mammalian system. As in human cells, 3′ uridylation of histone mRNA is induced upon replication arrest. Disruption of this 3′ tagging has a significant but limited effect on histone transcript regulation, consistent with multiple mechanisms acting to

regulate mRNA levels. Interestingly, 3′ end degraded transcripts are also subject to re-adenylation. Both mRNA pyrimidine tagging and re-adenylation are dependent on the same terminal-nucleotidyltransferases, CutA, and CutB, and we show this is consistent with the in vitro activities of both enzymes. Based on these data we argue that mRNA 3′ tagging has diverse and distinct roles associated with transcript degradation, functionality and regulation.

KEYWORDS

Aspergillus nidulans, histone, mRNA, nonsense-mediated decay, polyadenylation, pyrimidine

1 | INTRODUCTION

Post-transcriptional modification of mRNA has emerged as a key means of controlling functionality and expression (Nachtergaele and He, 2018). Amongst the wide range of modifications associated with the epitranscriptome is the cytoplasmic addition of non-templated nucleotides to the 3′ end of transcripts (Warkocki et al., 2018; Zigackova and Vanacova, 2018). The 3′ tagging of mRNA with a short run of pyrimidines (C + U), often precedes RNA degradation and translational repression. This was first observed for the non-adenylated human histone transcripts, where uridylation (3′ tagging with U) at the end of the S-phase or upon replication arrest was shown to be integral to cell cycle regulated transcript degradation (Lackey et al., 2016; Mullen and Marzluff, 2008). Subsequently, we and others have shown that in plant (*Arabidopsis thaliana*), fungal (*Aspergillus nidulans*, *Schizosaccharomyces pombe*) and human cells, polyadenylated transcripts are similarly tagged with U and/or C nucleotides (Chang et al., 2014; Morozov et al., 2010; 2012; Rissland and Norbury, 2009). The emerging data strongly indicate that 3′-pyrimidine tagging defines the point at which mRNA is earmarked for translational repression and degradation, thus establishing 3′-tagging as a novel component that determines transcript functionality. It has also been demonstrated that miRNA and siRNA from various species undergo tagging with non-templated nucleotides, primarily uridylation, to mark precursors for degradation (Zigackova and Vanacova, 2018). However, in some cases tagging regulates the maturation and activity of miRNAs and protects them from degradation (Morozov and Caddick, 2012).

For the non-adenylated human histone transcripts, 3′ uridylation is triggered within the cell cycle at completion of DNA synthesis and is coincident with accelerated transcript degradation and repression of histone production. Uridylation of the histone transcripts requires the RNA helicase, Upf1 (Kaygun and Marzluff, 2005a), which also plays a central role in nonsense-mediated mRNA decay (NMD), the cytoplasmic quality control mechanism which silences transcripts once the ribosome encounters an in-frame premature termination codon (PTC) (Celik et al., 2017). Upf1 is likely to alter the RNA-protein interactions and this may be critical both for the initiation

of 3′ degradation and tagging of the histone transcripts (Choe et al., 2014).

We have previously shown that both normal transcripts with shortened poly(A) tails and aberrant transcripts containing a PTC, undergo 3′-pyrimidine tagging in *A. nidulans* (Morozov et al., 2010; 2012) which is consistent with subsequent findings in mammalian systems (Chang et al., 2014; Kurosaki et al., 2018). With respect to *A. nidulans*, in both instances Upf1 is involved in the regulation of tagging (Morozov et al., 2012). The enzymes that catalyse addition of non-templated pyrimidines in *A. nidulans* are the terminal-nucleotidyltransferases, CutA, and CutB (Morozov et al., 2010; 2012). For wild-type (WT) transcripts, tagging with C and U nucleotides is initiated once the poly(A) tail is shortened to ~15 nucleotides, thus coupling poly(A) tail length surveillance to transcript degradation and translational silencing. Interestingly the data from high throughput sequencing of the 3′ ends in the human transcriptome reveal that pyrimidine tagging also occurs predominantly on transcripts with short (<25nts) poly(A) tails (Chang et al., 2014). This is consistent with A_{25} being the threshold length at which deadenylation triggers decapping in human cells and suggests that pyrimidine tagging plays a central role in this process.

In fungi, histone transcripts are adenylated, unlike the cell cycle regulated mammalian counterparts. To determine if cell cycle regulation of histone encoding transcripts in fungi involves a similar mechanism to that described in human cells, we investigated the role of mRNA tagging and the NMD component, Upf1, in *A. nidulans*. Hydroxyurea (HU), which inhibits DNA replication and blocks the cell cycle, represses histone transcript levels and induces high levels of uridylation at the 3′ end of the histone H2A encoding transcript. This uridylation is mediated by CutA and CutB. A range of factors involved in NMD, mRNA decapping, and both 5′ and 3′ transcript degradation are implicated in the regulatory response. One such factor, Upf2/NmdA, distinguishes the fungal machinery from that characterized in human cells. Additionally, we determined that 3′ end degraded transcripts can be re-adenylated, and this is also dependent on CutA and CutB. Our in vivo data are consistent with our in vitro analysis of CutA and CutB, which are shown to mediate both pyrimidine tagging and polyadenylation.

2 | RESULTS

2.1 | Blocking DNA synthesis leads to repression of histone transcript levels

In mammalian systems the histone encoding transcripts which are not polyadenylated are subject to cell cycle regulation, such that transcript levels drop once DNA synthesis is complete at the end of S-phase or is blocked by chemical treatment. This repression involves 3′ uridylation which promotes both decapping, through recruitment of the cytoplasmic Lsm1-7-Pat1 complex, and 3′–5′ degradation via the action of 3′hExo/Eri1 and the exosome (Hoefig et al., 2013; Marzluff and Koreski, 2017). In *A. nidulans* two nucleotidyltransferases, CutA and CutB, have previously been shown to

promote the degradation of oligo-adenylated ($\sim A_{15}$) transcripts via the addition of C and U nucleotides at their 3′ end (Morozov et al., 2010; 2012). One possibility being that 3′ tagging promotes the recruitment of the Lsm1-7 complex, leading to decapping, and 5′–3′ transcript degradation. The similarity between the two scenarios led us to test if histone transcripts in *A. nidulans*, which are polyadenylated, are subject to similar regulation via 3′ tagging.

To determine if *A. nidulans* histone mRNA levels are regulated in response to the repression of DNA synthesis we tested the effect of HU treatment on transcript levels using quantitative northern analysis. From these data (Figure 1) it is apparent that in the WT, levels of the histone H2A (*ht2A*, AN3468) and H3 (*ht3A*, AN0733) transcripts were significantly ($p < .05$) repressed by the addition of HU. In *A. nidulans rnrA* (AN0067) encodes a putative ribonucleotide
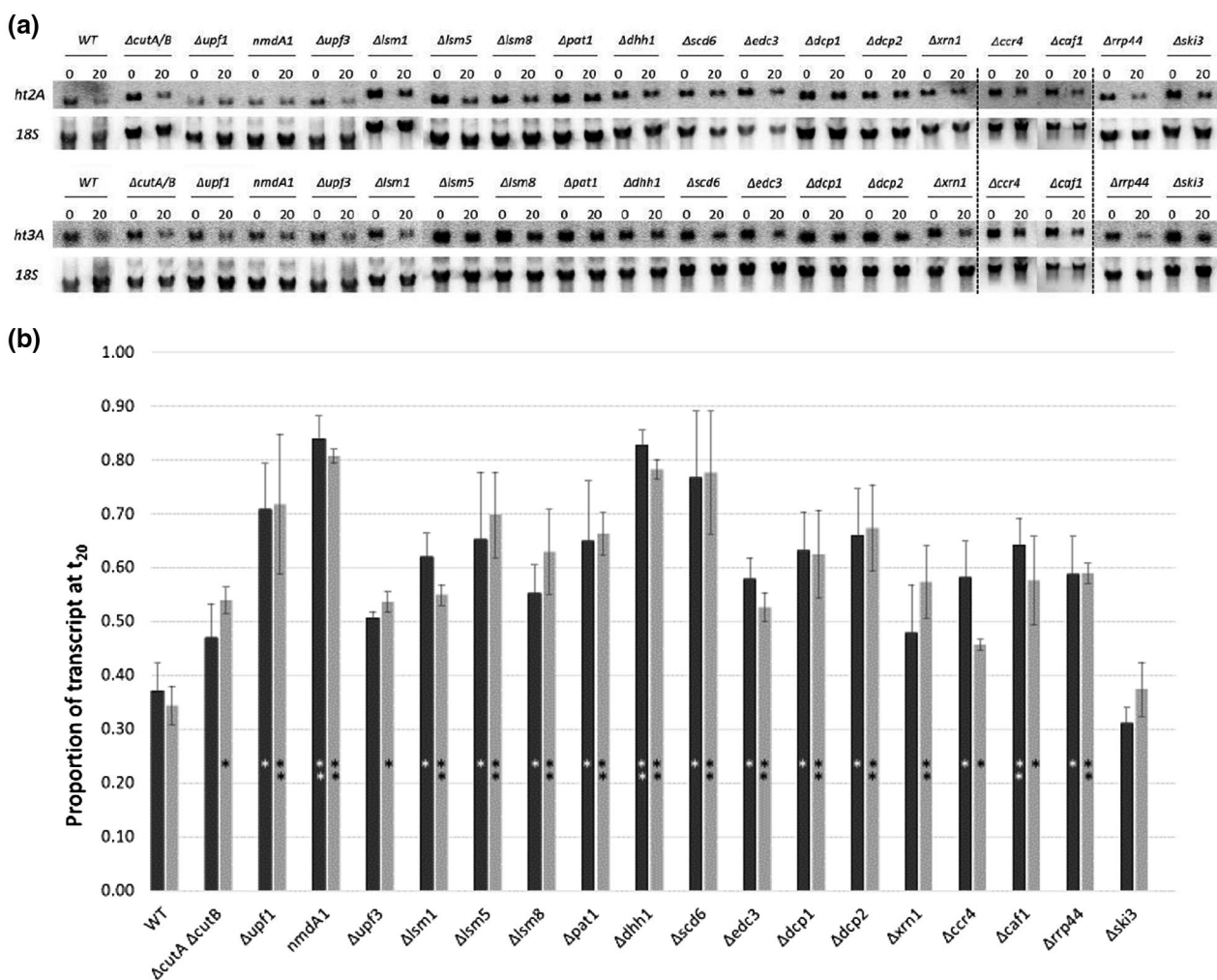
FIGURE 1 The HU induced response of histone transcript levels for a panel of RNA degradation mutants. (a) Quantitative northern blot analysis of the regulatory response to HU treatment of the *ht2A* and *ht3A* transcripts was conducted for wild type (WT), Δ*cutA* Δ*cutB*, Δ*upf1*, *nmdA1*, Δ*upf3*, Δ*lsm1*, Δ*lsm5*, Δ*lsm8*, Δ*pat1*, Δ*dhh1*, Δ*scd6*, Δ*edc3*, Δ*dcp1*, Δ*dcp2*, Δ*xrn1*, Δ*ccr4*, Δ*caf1*, Δ*rrp44*, and Δ*ski3* strains. Transcript levels were monitored immediately prior to HU treatment and after 20 min. 18S rRNA was used as a loading control. With the exception of Δ*ccr4* and Δ*caf1* (highlighted by hatched lines) all samples were run on the same gel but the order has been rearranged to complement the text. (b) The regulatory response is presented for each strain as the proportion of transcript remaining at t_{20}: *ht2A* (black bar) and *ht3A* (grey bar). Each data point is the mean of a minimum of three independent biological replicates. Error bars represent standard error. Significant difference in comparison to the wild type is indicated by either * ($p \leq .05$) or ** ($p \leq .01$). All strains showed a significant reduction in *ht2A* and *ht3A* transcript levels in response to HU treatment ($p \leq .05$)

reductase small subunit, orthologues of which are regulated by the cell cycle (Elledge et al., 1993). However, the *rnrA* transcript was not downregulated by the addition of HU (Figure S1).

To determine if CutA and CutB are involved in this regulatory response we monitored transcript levels in the Δ*cutA* Δ*cutB* double mutant (Morozov et al., 2010; 2012). In the double mutant (Figure 1), repression of *ht2A* and *ht3A* in response to HU treatment appears to be less dramatic but in the case of *ht3A* it is significant ($p < .05$). In a separate series of experiments, we also showed that single mutants disrupting either *cutA* or *cutB*, also had a marginal but significant effect on the repression of *ht2A* in response to HU treatment (Figure S1). This suggests that 3′ modification is involved but not essential in regulating the level of histone encoding mRNA in response to the perturbation of DNA synthesis.

In human cells the NMD component Upf1 is directly involved in the regulation of histone mRNA degradation in response to HU treatment (Kaygun and Marzluff, 2005b; Mullen and Marzluff, 2008). This also appears to be the case in *A. nidulans*, as HU induced repression of both *ht2A* and *ht3A* was significantly diminished in the mutant strain deleted for *upf1* (Figure 1). This implicates Upf1 in the regulatory response, suggesting conservation with the mammalian system.

NMD is known to involve a number of factors in addition to Upf1 (Maquat, 2002). To determine if other NMD components also play a role in the regulation of histone transcript levels we tested strains disrupted for two additional NMD factors, *nmdA/upf2* (Morozov et al., 2006) and *upf3* (AN0505). In both cases, the mutant strains exhibited a diminished regulatory response, although the effect of Δ*upf3* was only significant for *ht3A*. These data implicate the full NMD complex in mediating this regulation which distinguishes it from mammalian systems (Kaygun and Marzluff, 2005a; Meaux et al., 2018). Formally, it is possible that the effects observed may be indirect with these mutants altering the function or expression of an effector involved in this response.

To further assess the involvement of specific RNA degradation mechanisms in histone mRNA regulation, we undertook to test the effect of mutations disrupting different components involved by identifying the appropriate *A. nidulans* orthologues and constructing strains deleted for the respective loci. The factors tested in this way were: the decapping factors Dcp1 (AN7746) and Dpc2 (AN10010), components of the active cytoplasmic LSM complex (Lsm1/AN6199, Lsm5/AN5679, and Pat1/AN2751) and the nuclear LSM complex (Lsm8/AN01119), factors which act downstream of the LSM-Pat1 complex to promote de-capping (Dhh1/AN10417, Scd6/AN1055, and Edc3/AN6893) as well as the 5′–3′ exonuclease (Xrn1/AN11052), a component of the 3′–5′ exosome (Rrp44/AN3657, Ski3/AN3014) and the two previously described major deadenylases (Ccr4 and Caf1) (Morozov et al., 2010). As can be seen (Figure 1) all the mutants retained a regulatory response to HU treatment but, with the exception of Δ*ski3*, this was attenuated with respect to the WT. The significant disruption of regulation in the Δ*lsm8* strain was surprising, as the orthologue in *S. cerevisiae* is nuclear and not cytoplasmic. However, the intracellular localization of Lsm8 has not been characterized in *A. nidulans* and it is also possible that loss of this

putatively nuclear Lsm protein will alter the intracellular distribution of other Lsm components and/or function of the cytoplasmic Lsm1-7 complex (Novotný et al., 2012). With respect to the wide range of mutants examined, these data demonstrate that a number of distinct RNA degradation mechanisms are involved in the HU-induced repression of histone transcript levels. This is similar to the situation in mammalian systems where both decapping and subsequent 5′–3′ degradation, as well as exosome-mediated 3′–5′ degradation, have been implicated (Slevin et al., 2014).

To test this further we constructed a series of double mutants. Based on this analysis (Figure 2), mutations which disrupt factors involved in NMD (Δ*upf1* or *nmdA1*) and decapping (Δ*dcp2*, Δ*pat1*, Δ*lsm1*, or Δ*lsm5*) are additive, leading to significantly greater disruption of the HU-induced regulatory response. This demonstrates that these two RNA degradation mechanisms are acting independently. As expected, combining mutations that disrupt decapping did not result in an additive effect (e.g., the double mutants Δ*lsm5* Δ*lsm8* or the triple mutant Δ*cutA* Δ*cutB* Δ*lsm1*). However, it should be noted that additivity was not observed in the double mutant Δ*dcp2* Δ*rrp44*, in which two distinct degradation mechanisms are disrupted, namely mRNA decapping and 3′ degradation mediated by the exosome.

2.2 | Histone mRNA modification

To assess directly if the histone transcripts were subject to 3′ tagging and if this correlates with HU induced repression of transcript levels, we undertook cRT-PCR and sequencing of *ht2A* mRNA (Morozov et al., 2010). In order to specifically analyse capped mRNA, we first dephosphorylated the RNA sample (to prevent de-capped and 5′ degraded mRNA with a free 5′ end being circularized by ligation) and subsequently treated with tobacco acid pyrophosphatase to remove the 5′ cap, allowing the capped RNA to self-ligate. For analysis of natively de-capped RNA we utilized untreated mRNA. In the WT background we observed uridylation of the *ht2A* transcript, with HU treatment resulting in higher levels of tagging (Figure 3, Table S1). In the absence of HU the vast majority of capped transcripts have a full 3′ UTR and the location of the poly(A) tail is in a narrow window. However, HU treatment leads to a broader distribution of 3′ ends, indicative of increased 3′–5′ degradation (Figure 3a). Additionally, an alternative poly(A) site, which occurs ~40 nucleotides upstream of the predominant poly(A) site, appears to be utilized in response to HU treatment (Figure 3b).

Pyrimidine tagging of *ht2A mRNA* differed from that described previously for other transcripts in *A. nidulans* (Morozov et al., 2010; 2012). First, it appears to be independent of poly(A) tail length (Figure 3a) which contrasts with its occurrence predominating when the poly(A) tail has been degraded to around A_{15} (Morozov et al., 2010). A previously described exception was observed for transcripts which are subject to NMD, where poly(A) tail length-independent tagging was observed (Morozov et al., 2012). Secondly, the vast majority of pyrimidine tags identified (52 of 55) were U specific, whereas previously both C and U nucleotides had been

FIGURE 2 Suppression of the histone transcript regulation in double mutants. (a) Northern blot analysis of the regulatory response of *ht2A* and *ht3A* transcripts to HU treatment for a range of double and triple mutant strains (Δ*upf1* Δ*lsm1*, Δ*upf1* Δ*lsm5*, Δ*upf1* Δ*pat1*, Δ*upf1* Δ*dhh1*, *nmdA1*Δ*lsm1*, Δ*cutA* Δ*cutB* Δ*lsm1*, Δ*lsm5* Δ*lsm8*, and Δ*dcp2* Δ*rrp44*). Transcript levels were monitored immediately prior to HU treatment (t_0) and after 20 min (t_{20}). The quantitative response of the histone transcripts, (b) *ht2A* and (c) *ht3A*, are presented for each strain as the proportion of transcript remaining at t_{20}. An Asterix (*) indicates a statistically significant ($p ≤ .05$) response to HU treatment, comparing transcript levels at t_0 and t_{20}, for the respective double or triple mutant. These data are arranged with the respective single mutants (or in the case of Δ*cutA* Δ*cutB* double mutant) each side of the double or triple mutant (hatched). Five of the double mutants (Δ*upf1* Δ*lsm1*, Δ*upf1* Δ*lsm5*, Δ*upf1* Δ*pat1*, Δ*upf1* Δ*dhh1*, and *nmdA1*Δ*lsm1*) did not show a regulatory response to HU treatment with respect to *ht2A* or *ht3A* transcript levels, suggesting almost complete ablation of the response. All the single mutants, the Δ*cutA* Δ*cutB* double mutant and wild type did show a significant response (Figure 1). Each data point is the mean of a minimum of three independent biological replicates. 18S rRNA was used as a loading control. Error bars represent standard error
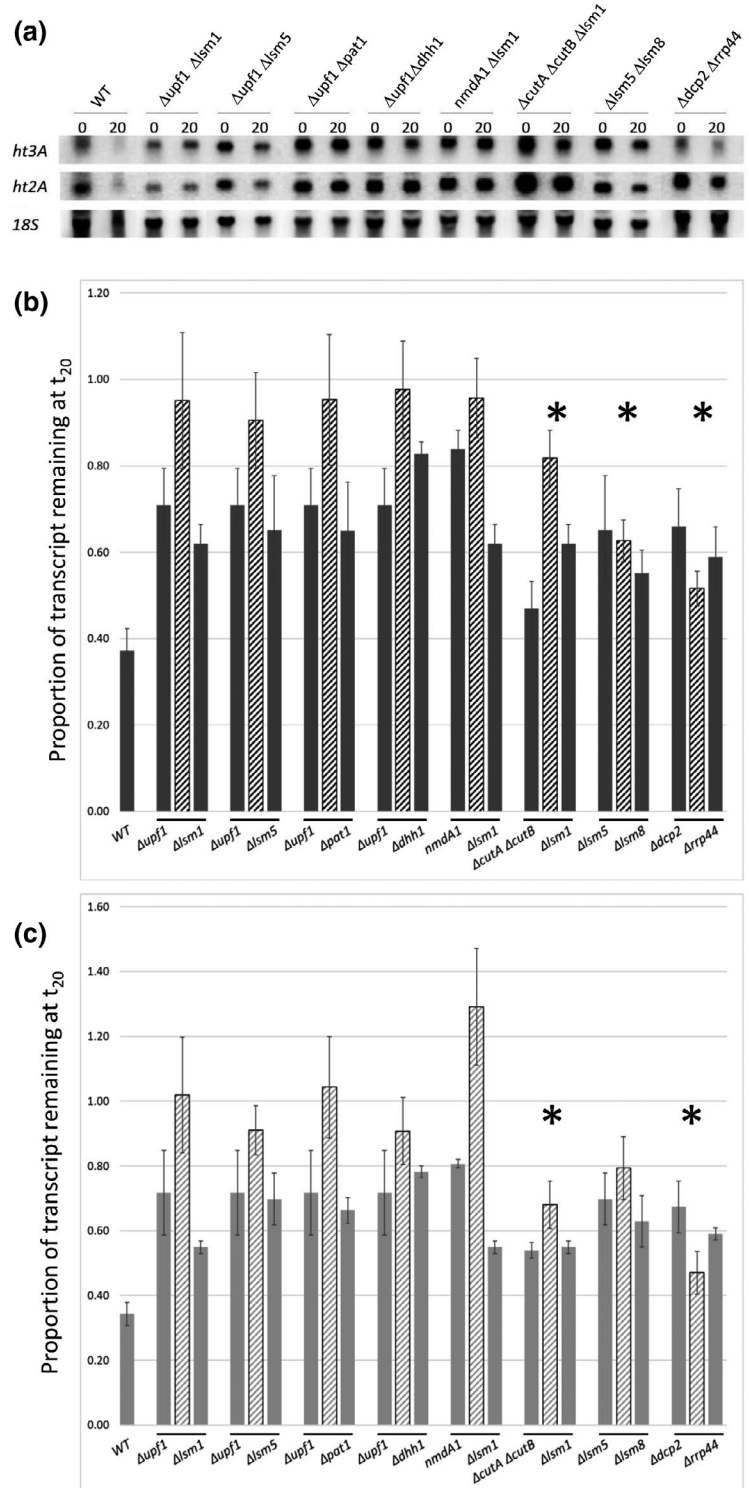
observed (Morozov et al., 2010; 2012). Rare instances of 3′ G tagging was also observed (three instances), including one which was extensive ($A_{19}G_{27}$). Finally, 3′ pyrimidine tagging of *ht2A* mRNA was predominantly associated with capped transcripts, which contrasts with the tagging observed previously for other transcripts (e.g., *gdhA* and *uaZ*; Morozov et al., 2010; Morozov and Caddick, 2012). However, this is similar to the situation in human cells, where a large proportion of tagged histone transcripts were shown to be capped;

mRNA uridylation being primarily associated with 3′ to 5′ degradation (Slevin et al., 2014).

ht2A 3′ tagging was not lost in strains disrupted for either *cutA* or *cutB* (Figure 3). However, the Δ*cutA* Δ*cutB* double mutant showed no tagging. The implication is that both enzymes are able to independently uridylate *ht2A* transcripts. In the Δ*upf1* strain, the frequency of tagging was also reduced for capped transcripts. The implication is that Upf1 promotes HU induced transcript uridylation,

possibly in a cap-dependent manner, as similarly observed for human histone mRNAs where Upf1 plays a major regulatory role (Mullen and Marzluff, 2008). This is also consistent with the high frequency of 3′ pyrimidine tagging observed for NMD substrates and the suppression of deadenylation-dependent 3′ tagging in Δupf1 strains (Morozov et al., 2012).

With respect to NMD, Upf1 activity is closely linked to translation. To determine if translation was required for HU induced uridylation we pre-treated the culture with cycloheximide as a translational inhibitor (Morozov et al., 2000), prior to HU treatment.

Under these conditions *ht2A* uridylation was drastically reduced (Figure 3, Table S1), consistent with translation being integral to tagging and Upf1 involvement. Finally, tagging was not apparently affected by deletion of *lsm5*.

2.3 | Transcript re-adenylation

Amongst the capped *ht2A* transcripts from the WT strain, expressed under different growth conditions (Figure 3b, Table S1),

(a)

(b)

WT Cap -HU   WT Dc -HU

WT Cap +HU   WT Dc +HU

*cutA*310 Cap +HU   Δ*cutB* Cap +HU

Δ*cutA&B* Cap +HU   Δ*upf1* Cap +HU

Δ*lsm5* Cap +HU   WT Cap +Cx +HU

Key: ■ - Site of 3′ tagging
       ✻ - Use of upstream poly(A) site
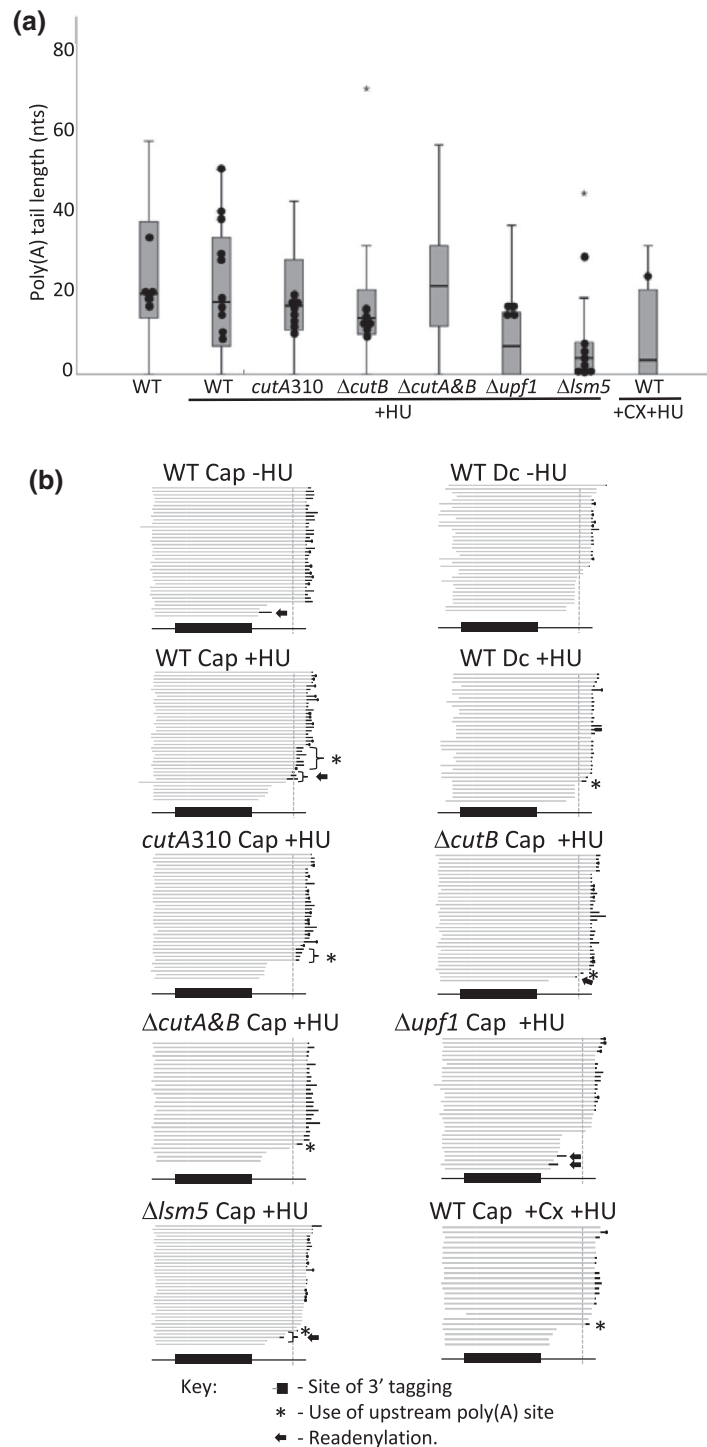   ← - Readenylation.

FIGURE 3 cRT-PCR analysis of ht2A mRNA. The addition of non-templated nucleotides to the 3′ end of the *ht2A* transcript in the wild-type (WT) and five mutant strains (*cutA*310, Δ*cutB*, Δ*cutA* Δ*cutB*, Δ*upf1* and Δ*lsm5*) was assessed by cRT-PCR. *cutA310* is point mutation which disrupts catalytic activity (Morozov et al., 2010). (a) The distribution of the poly(A) tail lengths for capped transcripts is displayed using a box plot with Turkey whiskers, where the top and bottom of the box represent limits of the upper and lower quartiles, with the median being indicated by the horizontal line which lies within the box. The whiskers show the highest and lowest reading within 1.5 times the interquartile range. Outliers are indicated [star]. Projected onto this is the distribution of clones that include 3′ uridylation [●]. Where indicated, cultures were treated with HU (+ HU), 20 min prior to harvesting, and cycloheximide (Cx), 10 min prior to HU treatment. For each strain and treatment, three separate samples were used and the combined data are presented. In the wild type the frequency of uridylation increases with HU treatment but the distribution relative to poly(A) tail length is very broad. Additionally, the Δ*upf1* strain showed low levels of uridylation and the Δ*cutA* Δ*cutB* did not show any. (b) The distribution of sequenced transcripts derived from the various strains and treatments are presented, with additional data in Figure S2. The locations of the 3′ and 5′ ends (grey line) and poly(A) tail (black line), and can be compared with the transcript model at the base of each set of data (with the thin line representing the UTRs and the thick line the ORF). We have indicated the sites of 3′ tagging with U, C, or G nucleotides (black box). Instances of polyadenylation at an upstream site observed specifically during HU treatment and putative instances of re-adenylation. Re-adenylation is suspected where the adenylation site is at least 50 nucleotides upstream of the principal poly(A) site, as delineated by the blue dashed line. A full summary of all relevant data, including sample numbers, is presented in Table S1

39 showed significant 3′ degradation (>50 nucleotides relative to the predominant poly(A) site). Of these seven (18%) were polyadenylated, with an average tail length of A_{34}. For the WT strain, none of the 16 decapped transcripts with extensive 3′ degradation had poly(A) tails, although one polyadenylated transcript was observed for the *cutA310* strain. Of the four capped *ht2A* transcripts derived from the Δ*cutA* Δ*cutB* double mutant that had extensive 3′ degradation, none were adenylated. Although this is very small sample number, these data may indicate that the two terminal transferases, CutA and CutB, catalyse re-adenylation of 3′ degraded transcripts.

To investigate the occurrence of putative re-adenylation events further we examined a range of other transcripts by 3′ adapter primer ligation (APL) (*niaA*, *niaD*), which allows the cloning and sequencing of 3′ ends, or by cRT-PCR (*gdhA*, *uaZ*), which provides sequence data for both the 5′ and the 3′ end of transcripts (Figures 4 and S2). With respect to the Δ*cutA* Δ*cutB* double mutant, of the 68 transcripts which showed significant 3′ degradation (<50 nts) none showed adenylation. For *niaA* and *niaD*, re-adenylation of transcripts was observed in the WT background for 3 of the 10 (30%) and 14 of the 23 (60%) degraded transcripts, respectively (Figure 4). However, no re-adenylation was apparent in either Δ*cutA* or Δ*cutB* single mutants or the double mutant. For the WT, of the 105 decapped *gdhA* transcripts analysed, 12 had significant 3′ degradation of which four (33%) contain long poly(A) tails, A_{80}, A_{53}, A_{28}, and A_{20}. Similarly, for 3′ degraded *uaZ* transcripts, re-adenylation was observed (Figure 4). Out of 49 capped *uaZ*+ mRNAs in the WT background one of the six transcripts with significantly degraded 3′ ends carried a 26-nucleotide poly(A) tail at the position −72 (33 nts downstream of the stop codon). Of the three de-capped *uaZ*+ transcripts that were re-adenylated two were also at position −72, with poly(A) tails of 19 and 21 nucleotides.

We hypothesized that the location of re-adenylation sites is likely to relate to the efficiency of 3′–5′ degradation, with recalcitrant sequences being more likely to be substrates for re-adenylation. In support of this hypothesis is the apparent non-random distribution of re-adenylation sites, with multiple examples of re-adenylation being observed at particular positions within transcripts

(Figure 4c). A possible basis for this is that these sites correlate with RNA sequences which form double stranded structures that could potentially inhibit exosome-mediated degradation. Based on this, re-adenylation may occur in order to assist in exosome-mediated degradation, as is known to be the case with oligoadenylation mediated by the TRAMP complex (Nousch et al., 2017). Alternatively, paused 3′ degradation may facilitate re-adenylation and the restoration of translation.

2.4 | In vitro analysis of CutA and CutB activity

Considering the in vivo data, which indicates that CutA and CutB are responsible for both mRNA 3′ pyrimidine (C + U) tagging and re-adenylation, we undertook to characterize the terminal ribonucleotidyl transferase activity for both CutA and CutB in vitro. Expression and purification of full-length CutA and CutB were complicated by the fact that both proteins are predicted to have extensive unstructured or disordered regions that flank a conserved and ordered central region that is responsible for the ribonucleotidyl transferase activity (Figure S3). Accordingly, a series of expression constructs with variable N and C termini (Figure S4a-b), which exclude these unstructured regions, were designed and screened to identify constructs that express well-folded protein. High-throughput screening, in collaboration with the Oxford Protein Production Facility (OPPF), identified a single well-expressing CutA clone, pOPINF-CutA(109-460) (N-terminally His6-tagged), which allowed for the subsequent purification of the conserved central catalytic core of CutA (Figure S4c). Although a suitable expression construct for CutB was not identified in the high-throughput screens, additional constructs were generated and screened manually where the clone pOPINF-CutB(248-694) (N-terminally His6-tagged) showed the best expression and solubility (Figure S4d). However, CutB(248-694) was generally unstable, rapidly degrading after affinity purification, limiting downstream analysis.

Consistent with CutA and CutB being responsible for both mRNA the addition of short 3′ pyrimidine tags and re-adenylation (Figures 3, 4 and S2; Table S1; Morozov et al., 2010; 2012), it has
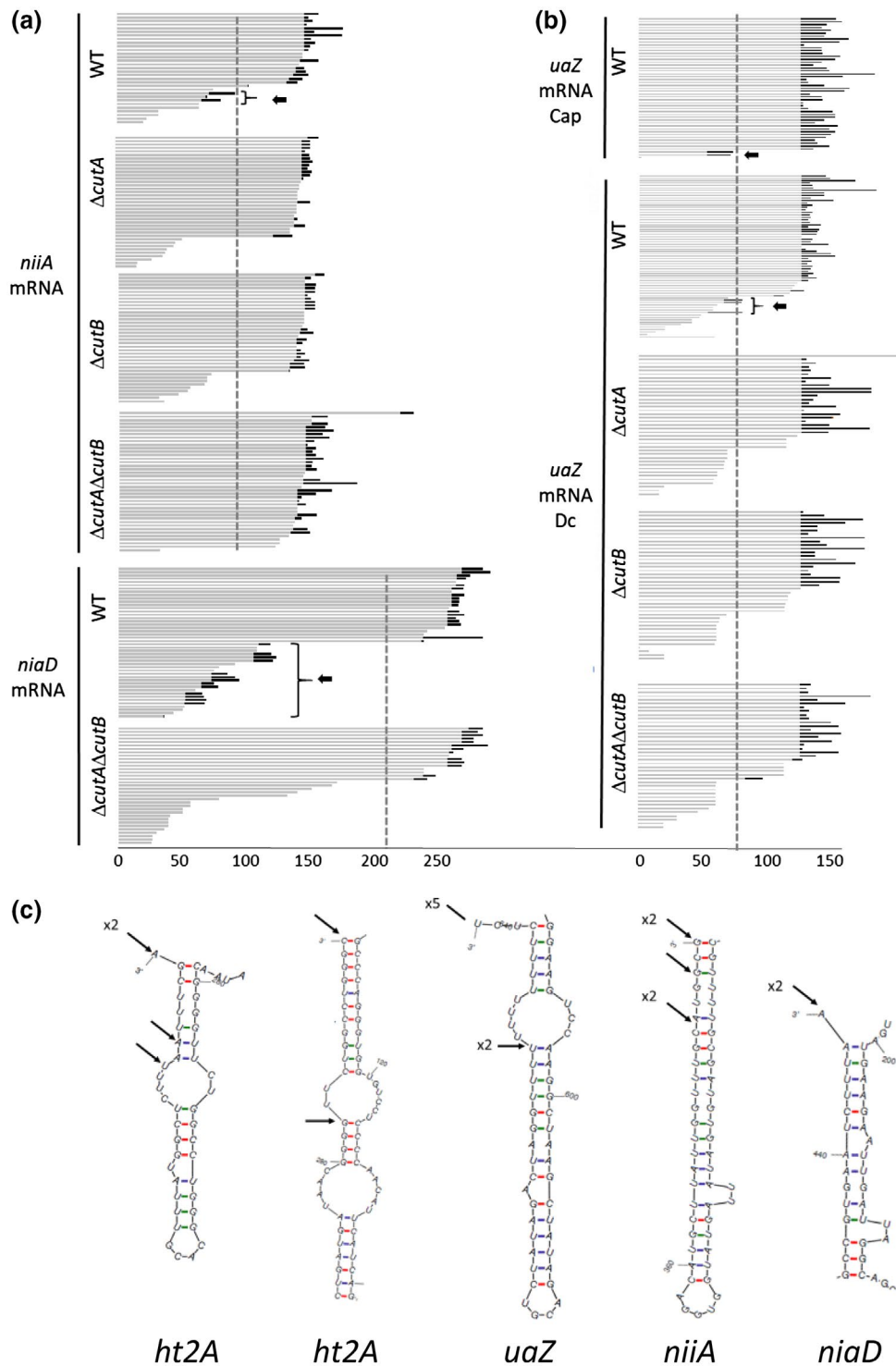
FIGURE 4 Distribution of putative re-adenylation sites. Examples of mRNA 3′ ends (grey line) and poly(A) tails (black line) with the putative re-adenylation sites indicated (arrow) in wild-type (WT) and mutant strains (Δ*cutA*, Δ*cutB* and Δ*cutA* Δ*cutB*) using (a) APL for *niiA* and *niaD* transcripts or (b) cRT-PCR for both capped (Cap) and decapped (Dc) *uaZ* transcripts. Additional cRT PCR data are presented in Figure S2. (c) Examples of re-adenylation locations are given for *ht2A*, *uaZ*, *niiA*, and *niaD*, as indicated with an arrow. Where multiple examples were identified at the same location the number of occurrences is indicated. These RNA sequences are represented as mFOLD (Zuker, 2003) secondary structure predictions

been observed that proteins belonging to the same class of terminal nucleotidyl transferase have a range of nucleotide preferences (Norbury, 2013). To determine the nucleotide specificity of

CutA(109-460) and CutB(248-694) we used a gel-based assay to monitor nucleotide addition to a short fluorescein labeled RNA oligonucleotide (A_{15}) designed to mimic the poly(A) tail. As seen

in Figure 5a, incubation of CutA(109-460) in the presence of ATP resulted in extensive polyadenylation of the RNA oligonucleotide (A$_{15}$) with tails of >40 nucleotides. Similarly, in the presence of UTP and CTP (Figure 5a), CutA catalysed the non-templated extension of the RNA substrate, however, the extent of the reaction was much less when compared to ATP. In the presence of UTP, CutA(109-460) extended >95% of the RNA substrate by 1–20 nucleotides while in the presence of CTP tagging activity was lower with >95% of the substrate being extended by one to four nucleotides after 60 minutes (Figure 5a). In the presence of GTP, CutA showed limited activity with <5% of the A$_{15}$ substrate being extended after 60 minutes.

In the case of CutB its lower yield and general instability limited extensive analysis. However, when compared to CutA at a single time point (5 min) both proteins showed ribonucleotidyl transferase activity in the presence of ATP, UTP, and CTP and minimal activity with GTP (Figure 5b). To exclude the possibility that the observed activity resulted from a co-purifying contaminant, catalytically inactive variants of CutA(109-460) and CutB(248-694) were constructed by introducing mutations into both genes which substituted alanine for the aspartic acid residues putatively involved in coordinating magnesium ions within the catalytic centre (Stagno et al., 2007), yielding the single mutants CutA(D214A), CutA(D216A), and the double mutant CutB(D314A D316A). Loss of function has previously
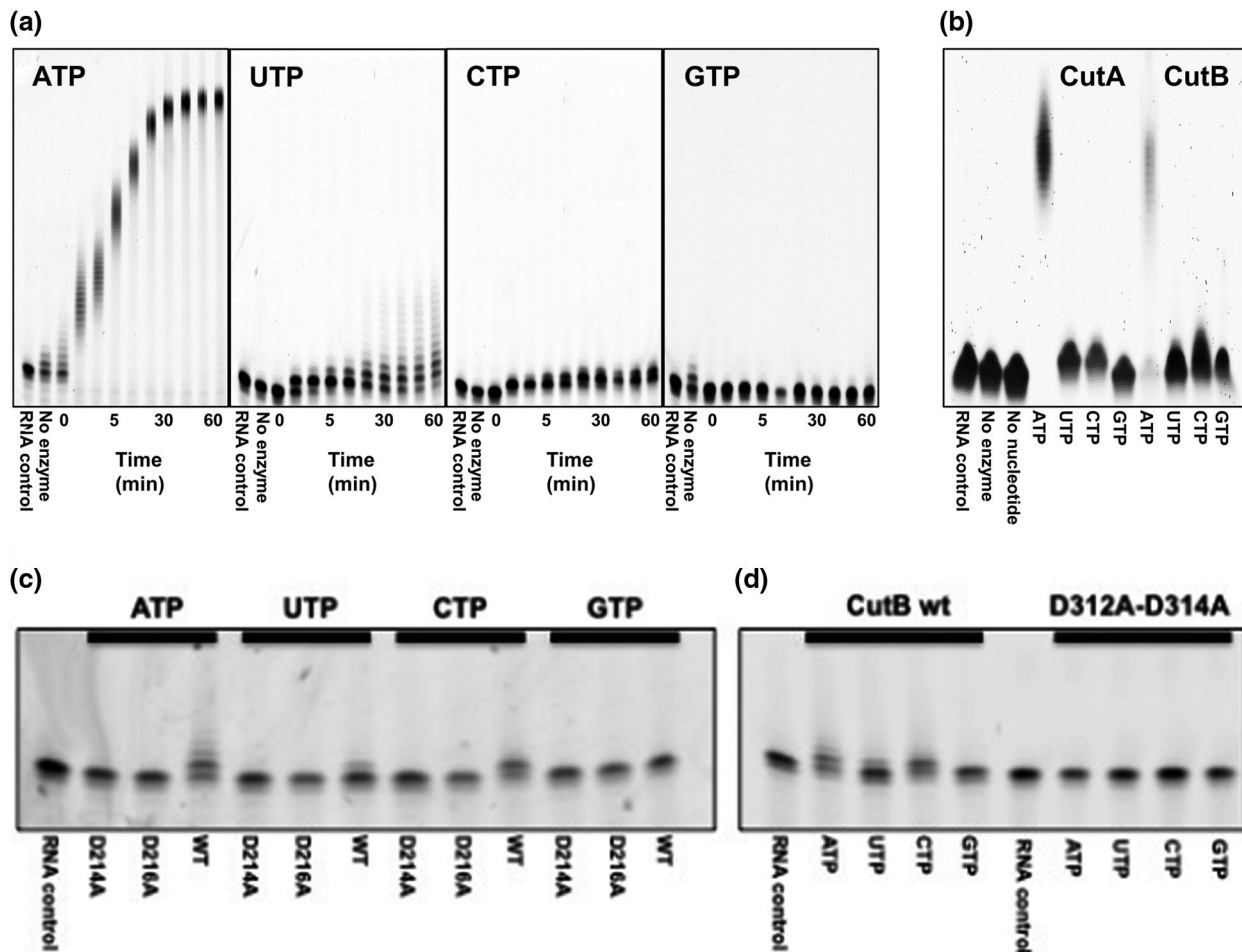

FIGURE 5 Characterisation of CutA(109-460) and CutB(248-694) nucleotidyl transferase activity in vitro. (a) The nucleotide specificity of CutA(109-460) was determined by assaying the non-templated extension of a fluorescein labeled RNA oligonucleotide (A$_{15}$) on a 15% polyacrylamide/7M urea gel. The reactions were initiated with 2.5 µM CutA(109-460), 10 µM A$_{15}$ oligonucleotide, and with individual NTPs (0.5 mM) as indicated in panel. Reactions were incubated at 20°C for the indicated time (0–60 min). (b) The nucleotide specificity of CutA(109-460) and CutB(248-694) were compared using an assay as described in panel A. Due to the instability of CutB, the assay was carried out at a single time point (5 min, 20°C) using protein (2.5 µM) directly after Ni-affinity purification. The assay was carried with 50 µM A$_{15}$ oligonucleotide, and with individual NTPs (0.5 mM) as indicated in panel. Aspartic acid residues putatively involved in coordinating magnesium ions within the catalytic centre (Stagno et al., 2007) were substituted for alanine residues generating the single mutants CutA(D214A), CutA(D216A) and the double mutant CutB(D314A D316A). The effect of these mutations on the nucleotidyl transferase of (c) CutA(109-460) and (d) CutB(248-694) was determined by assaying the non-templated extension of a fluorescein labeled RNA oligonucleotide (A$_{15}$). The reactions were initiated with either 2.5 µM of wild-type (WT) or mutant (D214A or D216A) CutA(109-460, D214A) or wild type or mutant (D312A-D314A) CutB(248-694) (directly after Ni-affinity purification) and 50 µM ATP, UTP, CTP, or GTP, as indicated

been confirmed for the two CutA substitutions in vivo (Morozov et al., 2012). These mutant proteins were all shown to be inactive (Figure 5c,d), confirming that the observed nucleotidyl transferase activity originates from the WT CutA(109-460) and CutB(248-694) constructs. Accordingly, the in vitro results indicate that CutA and CutB harbor adenylation, uridylation, cytidylation activities, which is fully consistent with the in vivo data, suggesting both proteins play a role in transcript re-adenylation and transcript 3′ pyrimidine (C + U) tagging.

Our current in vivo analysis of histone transcripts (Table S1) and prior analyses of transcripts not subject to NMD (Morozov et al., 2010) indicate different tagging activities; only uridylation is observed in the former while a mixture of C/U tags are observed in the

latter. Accordingly, to understand how the isolated catalytic domain of CutA and CutB behave in our in vitro assays, we compared the affinity of CutA(109-460) for CTP and UTP by monitoring the addition of single C or U residues to the A_{15} substrate, under a range of NTP concentrations, and determining the kinetic parameters, K_m and K_{cat}, of the ribonucleotidyl transferase reaction. As seen in Figure 6, CutA(109-460) with the A_{15} substrate required higher UTP concentrations to achieve turnovers comparable to that achieved with CTP; for example, at 4 µM CTP ribonucleotidyl transferase activity was readily observed while at 7.5 µM UTP only slight uridylation of the transcript is present. Quantitation of these results indicates that CutA(109-460) with the A_{15} RNA oligonucleotide has a higher affinity for CTP, that is, the K_m for UTP was ~45-fold higher than for

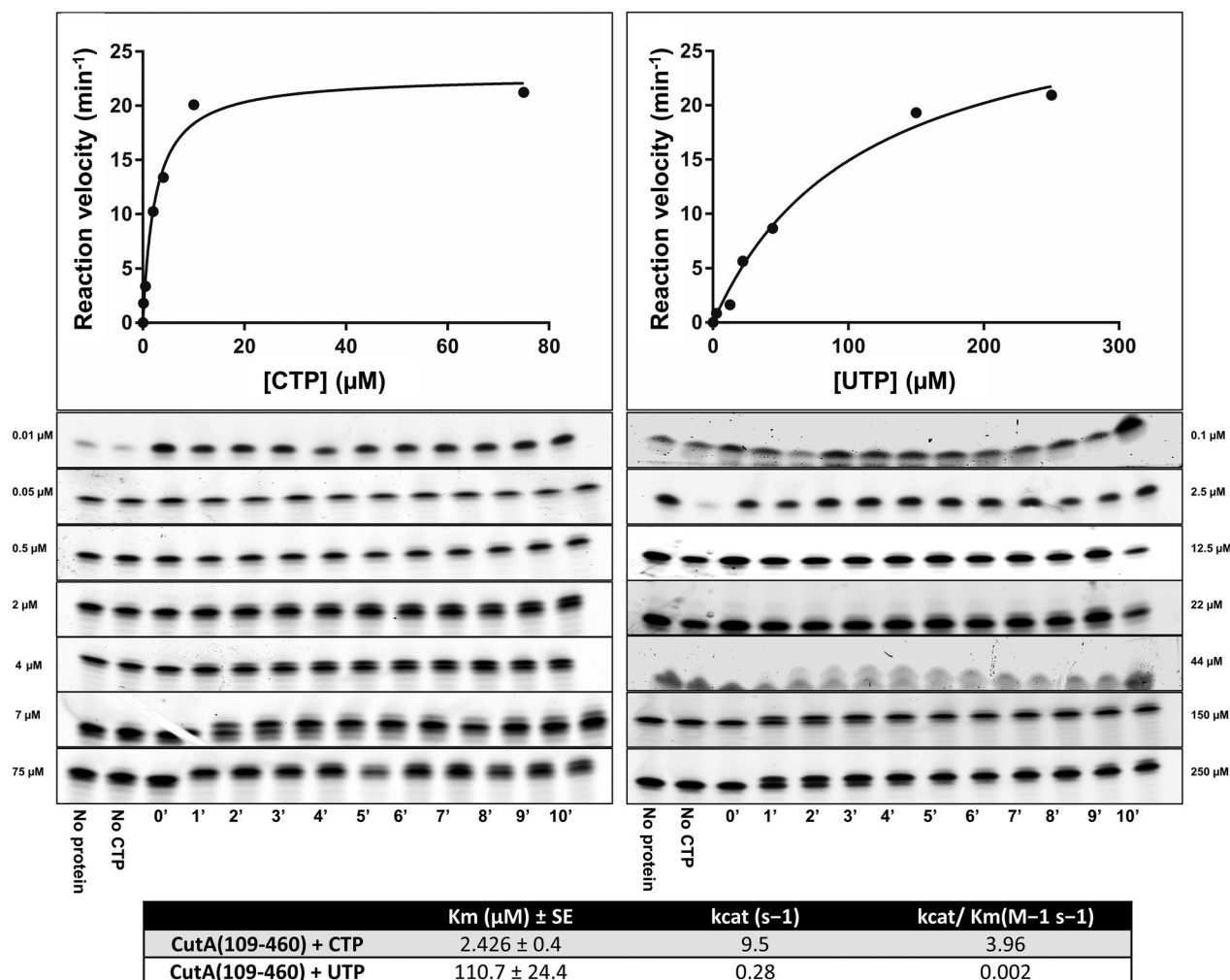|	Km (µM) ± SE	kcat (s−1)	kcat/ Km(M−1 s−1)
CutA(109-460) + CTP	2.426 ± 0.4	9.5	3.96
CutA(109-460) + UTP	110.7 ± 24.4	0.28	0.002

FIGURE 6 Kinetics analysis of CutA(109-460) cytidylation and uridylation activity. The non-templated cytidylation (a) or uridylation (b) of a fluorescein labeled A_{15} RNA oligonucleotide was assayed under conditions favoring the addition of a single nucleotide to the terminal A residue. Accordingly, reactions were initiated with 2.5 µM CutA(109-460), 10 µM A_{15} oligonucleotide and either UTP or CTP at the indicated concentrations. The individual reactions were incubated, for the time shown in the panels, at 20°C before terminating the reaction and analysing the products on a 15% polyacrylamide/7M urea gel. Subsequently the intensity of the +1 bands (i.e., where one nucleotide had been added) were determined using the Imagequant software package and the fraction of product formation over time was plotted for each reaction at a given nucleotide concentration, allowing one to determine the relative velocity of every reaction at a given NTP concentration. Subsequently these rates were plotted and the kinetic parameters describing the cytidylation and uridylation activity of CutA(109-460) on a A_{15} RNA oligonucleotide were calculated using GraphPad (Prism7 software) according to the Michaelis Menten equation and are shown in the table

CTP, and the catalytic efficiency of CutA(109-460) with CTP was higher than observed for UTP (Figure 6). This preference of CutA for CTP is consistent with a similar characterization of CutA reported by Kobylecki and colleagues (Kobylecki et al., 2017), but different to that seen in Table S1 where uridylation is largely observed in vivo, possibly indicating in the higher availability of UTP in vivo.

Interestingly, as seen in Figure 5a, with CutA the 3′ tags are longer with UTP than with CTP, indicating that the terminal residue of the RNA oligonucleotide may influence the activity of both CutA and CutB. Therefore, we compared the effect of the 3′ terminal nucleotide on the ribonucleotidyl transferase activity of CutA and CutB by assaying 3′ tagging of an RNA oligonucleotide in which the terminal residue is varied.

In Figure 7, it is most evident when adenylation activity is compared, CutA(109-460) and CutB(248-694) exhibit different activity profiles, namely CutB(248-694) extensively adenylates all substrates regardless of the terminal nucleotide while CutA(109-460) only shows adenylation activity when the substrate oligonucleotide harbors a terminal A or G residue. Moreover, with both proteins the uridylation and cytidylation activities are weakest when the terminal residue of the RNA oligonucleotide substrate is a C. A detailed in vitro analysis of CutA activity has been published (Kobylecki et al., 2017). This is expanded on here, where we compare the activity profiles of CutA and CutB, and measure activity when the terminal residue of the substrate RNA is a G. Similar to our observations, Kobylecki et al. (2017) reported that CutA had low activity when the terminal residue in the substrate was a C, although they did not observe an inhibitory effect when the terminal residue was a U. This difference could be attributed to the precise nature of the RNA substrates or the exact CutA constructs used. Importantly here it is demonstrated

that although CutA and CutB have overlapping activity profiles, the adenylation activity of CutB(248-694) is not dependent on the nature of the terminal residues in the RNA substrates suggesting that CutB could have a distinct role in vivo that requires more robust adenylation activity. In the case of CutA the limited adenylation activity when the terminal residue is a C or U may serve to clearly delineate the adenylation and uridylation activities such that when required CutA can effectively promote addition of poly-U tails to transcripts as seen for the histone transcripts (Figure 3 and Table S1).

3 | DISCUSSION

The cell cycle regulation of histone encoding transcripts is well described in metazoans (Marzluff and Koreski, 2017). A key aspect is regulated transcript degradation which occurs at the end of S-phase, when DNA replication is complete. The same response can also be induced by blocking DNA replication chemically. This regulatory process involves the unique 3′ stem-loop structure, instead of the poly(A) tail and is specific to the cell cycle regulated histone transcripts. This structure is bound by SLBP which is critical for RNA maturation, stability and translation. As such the SLBP plays a role like that of the poly(A) binding protein in more conventional eukaryotic transcripts which are polyadenylated. Cell cycle regulation of histone transcript stability is known to be translation dependent (Graves and Marzluff, 1984; Slevin et al., 2014), involve the RNA helicase Upf1 (Kaygun and Marzluff, 2005a) and 3′ uridylation of the mRNA is integral to the regulatory process (Mullen and Marzluff, 2008). Although fungal histone coding transcripts are polyadenylated, the coincidence of 3′ pyrimidine tagging at the point when deadenylated transcripts are
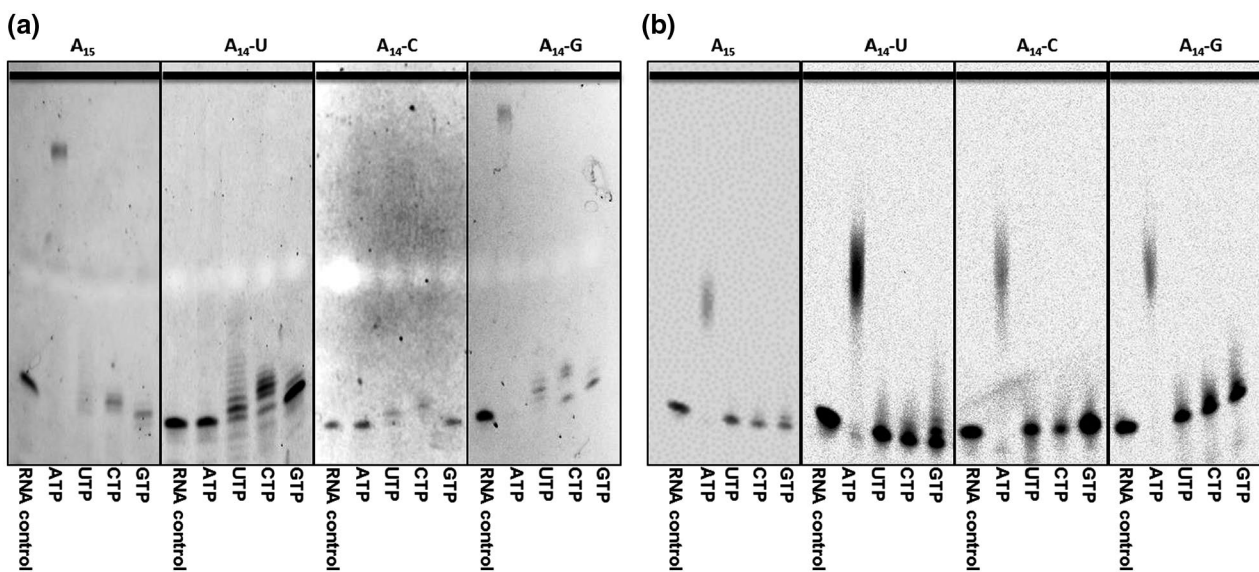
FIGURE 7 The effect of the RNA substrate's terminal nucleotide on the in vitro nucleotidyl transferase activity CutA(109-460) and CutB(248-694). The ability of CutA(109-460) and CutB(248-694) to promote the non-templated extension of a fluorescein labeled RNA oligonucleotide, when the terminal residue is varied, was assayed by conducting reactions with (a) 2.5 μM CutA(109-460) and (b) CutB(248-694) directly after Ni-affinity purification, 0.5 mM NTPs (as indicated in panel), and 10 μM of either A_{15}, A_{14}-U, A_{14}-C and A_{14}-G RNA oligonucleotides. Representative images are presented from triplicate (CutA) and duplicate (CutB) experiments. Reactions were incubated at 20°C for 30 min for CutA and 10 min for CutB

decapped and degraded in *A. nidulans* and the previously identified link between Upf1 and 3′ tagging (Morozov et al., 2012), led us to examine if a similar cell cycle dependent regulatory mechanism was involved in regulating histone transcripts.

From our data it is clear that in *A. nidulans* levels of both H2A and H3 encoding transcripts are downregulated in response to HU treatment, which is known to block DNA synthesis and trigger the repression of histone transcript levels in metazoans (Kaygun and Marzluff, 2005a; Koc et al., 2004). In *A. nidulans* this response is partially suppressed in mutant strains disrupted for the NMD factor, Upf1, and the two nucleotidyl transferases, CutA and CutB, which are required for pyrimidine tagging. These results mirror those for mammalian cells. However, one intriguing difference is that in *A. nidulans* two additional NMD factors tested, Upf2 and Upf3, are also involved in this regulatory process, as disruption of the respective genes also partially suppresses the HU response. In mammalian cells the only NMD factor implicated is Upf1 (Kaygun and Marzluff, 2005a) and it has been suggested that its RNA helicase activity may act to displace SLBP, independently of the other NMD factors (Marzluff and Koreski, 2017). In mammals, there are various histone paralogues; regulation by the cell cycle is specific to the major forms which all have the stem-loop structure in place of the poly(A) tail. Our data suggest that this regulatory mechanism, involving Upf1 and transcript uridylation, predates the emergence of this unusual histone specific 3′ end processing mechanism. Presumably, in animals the histone paralogues that encoded polyadenylated transcripts, subsequently lost this regulatory mechanism, liberating them from cell cycle regulation. However, it should be noted that in *C. elegans* some polyadenylated histone transcripts retain cell cycle regulation (Sanicola et al., 1990).

In support of HU induced repression of *ht2A* and *ht3A* mRNA levels being at least in part effected by RNA degradation, mutations disrupting a range of factors involved in RNA degradation led to partial suppression of this HU response. These data implicate decapping, deadenylation, and both the 5′–3′ and 3′–5′ decay pathways in the regulation of histone expression in response to HU. Inactivation of no single RNA degradation factor or pathway fully suppressed this regulatory response. However, strains combining mutations which are known to disrupt NMD (Δ*upf1* or Δ*nmdA1*) with those disrupting components of the Lms1-7-dependent decapping pathway (Δ*lsm1*, ΔΔ*lsm5*, Δ*pat1* or Δ*dhh1*) were additive, resulting in full suppression of the response to HU treatment. These data argue for at least two parallel mechanisms, the Lsm1-7 decapping pathway and a second involving NMD components, acting independently to effect the histone regulatory response to HU induced disruption of the cell cycle.

The known involvement of uridylation in cell cycle-mediated regulation of mammalian histone transcripts and our observation that when the terminal transferases, CutA and CutB, are disrupted in *A. nidulans* the response to HU treatment is partial suppressed, strongly support the proposal that pyrimidine tagging is integral to this regulatory mechanism in *A. nidulans* and again suggests conservation across the kingdoms. Furthermore, analysis of histone mRNA 3′ tagging demonstrated that in *A. nidulans* the *ht2A* transcript is uridylated in actively growing cells and the frequency of this

3′ tagging increases in response to HU treatment. Assuming *ht2A* 3′ tagging is cell cycle specific, we would expect a low transient level of tagging to occur throughout a population of cells. HU treatment should increase the proportion of cells in which DNA synthesis is blocked, and thus increase uridylation if it occurs within the cell cycle at the end of S-phase. Our data fully support these assumptions.

We have shown that in *A. nidulans* 3′ tagging of *ht2A* mRNA is dependent on *cutA* and *cutB*, with the double mutant, Δ*cutA* Δ*cutB*, showing no tagging, although only a marginal reduction in tagging is observed in the respective single mutants. This indicates that CutA and CutB are both able to mediate *ht2A* tagging. In the Δ*upf1* strain *ht2A* 3′ tagging was reduced, implicating this NMD component in either facilitating or regulating tagging, as is also observed in human cells and for other *A. nidulans* transcripts (Kaygun and Marzluff, 2005a). It has been suggested that this relates directly to the RNA helicase activity of Upf1 which may displace bound proteins, making the RNA more accessible to 3′ modification (Choe et al., 2014). Alternatively, Upf1 may directly recruits the terminal transferases to specific transcripts and/or activates them at particular mRNAs.

Previous analysis of various transcripts in *A. nidulans* showed 3′ pyrimidine tagging involves both C and U nucleotides. As the observed *ht2A* mRNA tagging was predominantly U specific, this regulatory response appears distinct from deadenylation specific and NMD induced tagging described previously (Morozov et al., 2010; 2012). Second, the occurrence of tagging appears to be widely distributed with respect to poly(A) tail length, unlike the previously described deadenylation length-dependent decapping, which is predominantly associated with short poly(A) tails of ~A_{15} (Morozov et al., 2010). The diversity of poly(A) tail lengths associated with histone mRNA tagging (Figure 3 and Table S1) implies that tagging is not being triggered by poly(A) tail length but by an independent regulatory mechanism responding to the cell cycle. A further difference, is that the majority of tagged *ht2A* transcripts were capped and not decapped. Tagging of capped transcripts is consistent with the data of Kaygun and Marzluf (Kaygun and Marzluff, 2005b) which show that uridylation of histone transcripts in mammalian cells occurs during translation. The hypothesis that mRNA 3′ tagging is initiated during translation, is also supported by our previous data (Morozov et al., 2012). Additionally, we found that pre-treatment with cycloheximide, which blocks translation by inhibiting elongation, dramatically reduced the level of *ht2A* mRNA tagging after HU treatment (Figure 3, Table S1), again implicating translation in mRNA 3′ tagging.

Recently, it has been shown that 3′ uridylation is a key step in the defence against RNA viruses, in both *C. elegans* and mammalian cells (Le Pen et al., 2018). The authors proposed that this tagging occurs in response to translation of the RNA genome. This link between RNA 3′ tagging and translation is fully consistent with NMD components having a key role in histone transcript uridylation, as observed in fungi and mammalian systems. It is also possible that translation is affected by tagging; our previous data indicated that efficient exclusion of NMD substrates from polysomes is dependent on 3′ tagging (Morozov et al., 2012). In HeLa cells, it was shown that during apoptosis removal of the tag by DIS3L2, but not the 3′ uridylation per se, leads to global

repression of translation, with depletion of DIS3L2 restoring translation (Thomas et al., 2015). The implication is that 3′ uridylation acts indirectly to repress translation of capped transcripts, possibly via the recruitment of DIS3L2 to the transcripts. As such cell cycle induced uridylation will act to repress histone expression more effectively than through accelerated transcript degradation alone.

A surprising novel observation was the apparent re-adenylation of transcripts which had undergone extensive (>50 nts) 3′ degradation. This putative cytoplasmic re-adenylation is dependent on CutA and CutB, with none being observed in the ΔcutA ΔcutB double mutant. The non-random distribution of re-adenylation events may correlate with RNA structure. One explanation would be that re-adenylation is associated with a cytoplasmic degradation mechanism similar to that proposed for uridylation of human cell cycle regulated histone transcripts (Hoefig et al., 2013), uridylation of transcripts during apoptosis (Thomas et al., 2015), nuclear adenylation mediated by the TRAMP complex (LaCava et al., 2005; Vanacova et al., 2005) and decay of bacterial ρ-independent transcripts (Cheng and Deutscher, 2005; Mohanty and Kushner, 2000). The nuclear TRAMP complex adds a short run of adenine nucleotides to promote 3′–5′ degradation (Fernandez-Moya et al., 2014; Nousch et al., 2017), particularly where the exosome is blocked by RNA structure (Pan et al., 2015). Cytoplasmic adenylation may play a similar role, potentially assisting the exosome in overcoming intransigent terminal 3′ RNA structures. It is pertinent to note that when cutB was originally identified, it was postulated that it would be a nuclear non-canonical poly(A) polymerase, equivalent Trf4p or Trf5p in S. cerevisiae (Pan et al., 2015).

An alternative function for re-adenylation could be the re-activation of translationally repressed transcripts which have undergone 3′ degradation but remained capped. It is also important to note that the possible extension of existing poly(A) tails would not have been identified in this study but may also occur. The cytoplasmic extension of poly(A) tails is a well-documented phenomenon in metazoans, particularly during development, where poly(A) shortening is used as a strategy to stabilize and translationally repress some transcripts and re-adenylation is used to activate them (Cui et al., 2013; Nousch et al., 2014; Radford et al., 2008; Subtelny et al., 2014). As the majority of re-adenylated ht2A transcripts was capped and the re-adenylation sites identified are within the 3′ UTR, it is possible that this activity re-activates partially degraded, translationally silent transcripts. However, there is a likely bias related to the location of the primers used for cRT-PCR and 3′ APL analysis. Finally, many of the transcripts have extensive poly(A) tails, which is not consistent with the TRAMP model, where oligoadenylation promotes degradation.

From this and previous studies a diversity of 3′ tags have been associated with CutA and CutB. These include short runs of C and/or U nucleotides (Morozov et al., 2010) and, in this study, adenylation. It was, therefore, important to confirm that these two enzymes have the relevant activities. Based on in vitro analyses of CutA and CutB, conducted both by ourselves and analysis of full-length CutA recently reported (Kobylecki et al., 2017), the two enzymes efficiently polyadenylated RNA substrates, consistent with the occurrence of some very long poly(A) tails associated with 3′ degraded transcripts. Both CutA

and CutB are able to add short tracts of C or U nucleotides. With respect to GTP, both CutB and CutA show marginal activity. Notably the terminal nucleotide of the RNA substrate is also important, with the 3′ nucleotide affecting activity; CutA cannot polyadenylate RNA if there is a terminal C or U residue, whereas CutB can polyadenylate all four classes of substrate (Figure 7) (Kobylecki et al., 2017). Additionally, adding a mixture of nucleotides to the in vitro reactions resulted in relatively short 3′ tails being synthesized compared to the situation where only ATP was added (data not shown). This would suggest that incorporation of a nucleotide other than an A, limits further extension. Kobylecki et al. (2017) observed that under such conditions the 3′ end had a bias for C, which may be explained by our observation that tagging activity with C is less extensive than with U. The extensive polyadenylation and the short pyrimidine tags reported in vivo may reflect differences in the intracellular concentration of the NTPs or regulation of CutA and CutB activity, possibility through interactions with other protein partners. One possibility is that interacting proteins, which may vary depending on the associated function, are able to alter the specificity of CutA and CutB and thus the functional signal associated with the 3′ tag, extending the repertoire and utility of these two enzymes.

This work describes three major findings. First, although fungal cell cycle regulated histone mRNAs are adenylated the key components and mechanism that regulated the histone transcript levels in response to the cell cycle are fundamentally conserved in fungi and mammalian systems. While there are many examples of conservation of this type, the striking aspect of this is that the divergence of mammalian histone 3′ ends, replacing the poly(A) tail with a stem-loop structure, has not been accompanied by an equivalent divergence in regulation. Second, we have shown that the nonsense-mediated RNA decay and the mRNA decapping pathways cooperate in the regulated repression of histone transcripts. Final, two new functions have been associated with the A. nidulans terminal transferases, CutA and CutB; they are directly implicated as a constituent of both the cell cycle histone regulatory mechanism as well as the more general cytoplasmic re-adenylation of partially degraded transcripts. This, combined with previously identified roles in deadenylation dependent decapping and NMD, indicates that these enzymes are likely to be modulated in multiple ways, and their activities modified to elicit different signals, contributing in distinct ways to the epitranscriptome.

4 | EXPERIMENTAL PROCEDURES

4.1 | A. nidulans strains and genetic techniques

A. nidulans markers and the genetic techniques used have been described previously (Clutterbuck, 1974; 1993). Growth media were as described by Cove (Cove, 1966). Strains deleted for dcp1/AN7746 and dpc2/AN10010, lsm1/AN6199, lsm5/AN5679, lsm8/AN01119, pat1/AN2751, dhh1/AN10417, scd6/AN1055, edc3/AN6893, xrn1/AN11052, rrp44/AN3657, ski3/AN3014 were constructed in A1149 (pyrG89; pyroA4; nkuA::argB) by direct transformation of recombinant

PCR constructs utilising *Aspergillus fumigatus pyrG* as the selectable marker, as described in (Szewczyk et al., 2006). Fidelity of the knockout strains was confirmed by PCR and Southern hybridization. Co-segregation of mutant phenotypes with the respective gene modification was confirmed by outcrossing. Strains bearing double or triple mutants were constructed by standard genetic crosses and had the following genotypes: $\Delta cutA$ $\Delta cutB$ $\Delta nkuA$, $\Delta upf1$ $\Delta lsm1$ $pantoB_{100}$, $\Delta upf1$ $\Delta lsm5$, $\Delta upf1$ $\Delta pat1$ uaZ_{14} $pantoB_{100}$, $\Delta upf1$ $\Delta dhh1$ $pyroA_4$, $nmdA1$ $\Delta lsm1$ $pantoB_{100}$, $\Delta lsm5$ $\Delta lsm8$, $\Delta dcp2$ $\Delta rrp44$ uaZ_{14} $pyroA_4$, and $\Delta cutA$ $\Delta cutB$ $\Delta lsm1$ $pyroA_4$.

4.2 | Transcript analysis

Growth of mycelia, RNA preparation, and quantitative northern analysis were as described previously (Caddick et al., 2006; Morozov et al., 2000). Briefly, 200 ml overnight cultures were incubated at 30°C for 14–16 h with shaking. Fully supplemented minimal media was used with 10mM either ammonium (for *ht2A* and *ht3*), nitrate (for *niiA* and *niaD*), or uric acid (for *uaZ*) as sole nitrogen source. Where required, hydroxyurea (1.5 mg ml^{-1}) was added to the cultures to inhibit DNA synthesis at t_0. Where required, proflavine (40 μg/ml) was used as a transcriptional inhibitor and cycloheximide (0.1 mg/ml) as a translational inhibitor, as described previously (Morozov et al., 2000; Platt et al., 1996). Circularised reverse transcriptase PCR (cRT-PCR) of *ht2A* mRNA was conducted according to Morozov et al. (2010). For the analysis of naturally decapped transcripts there was no pre-treatment of RNA. For capped transcripts, 25 μg of DNase I treated RNA was incubated with 5U of calf intestinal alkaline phosphatase in 25 μl of 1X CutSmart® Buffer (BioLabs) at 37°C for 15 min. Ten micrograms of chloroform/ethanol purified dephosphorylated RNA was treated with 2.5U of tobacco acid pyrophosphatase (TAP) in 20 μl of 1X TAP buffer at 37°C for 1 hour. All cDNA synthesis was carried out with SuperSrcipt reverse transcriptase following the manufactory protocol (Invitrogen). For *uaZ*, first-strand cDNA synthesis utilized oligonucleotide uaZ_5′RT (5′-CGGTCATTTCAGTGACGG-3′) and subsequent PCR was conducted using uaZ_5′RT and uaZ_3′For 5′-CAGACAAACCCTAACGGA-3′. For *H2A*, first-strand cDNA synthesis utilized oligonucleotides H2A_3′For1 (5′-AGAACCTCCTCCCCAAGAAG-3′) and H2A_5′RT (5′-GCCTTCGAAGAACGAGACTG-3′). For the naturally decapped samples PCR was conducted with a nested primer H2A_3′For2 (5′-GGCGTGGTTTGGTTCTCTTA-3′) and H2A_5′RT. For 3′ adaptor primer ligation (APL) 10 μM 5′ adenylated (5rApp-) adaptor (5′-GACTGGAATTCTCGGGTGCCAAGGC-3′) was ligated to the 3′ end of 1μg/μl total RNA using 40 u/μl AIR ligase in AIR ligase buffer (Bioo Scientific) and 10% PEG-8000 at 25°C for 2 hrs. Adaptor ligated RNA was cleaned by RNA clean & concentrator kit (Qiagen). For the *niiA* and *niaD* genes, first-strand cDNA synthesis was performed using 70 ng/μl of the adaptor ligated RNA, 10 μM RT primer (5′-GCCTTGGCACCCGAGAAT-3′) and 200U/μl of SuperScript II reverse transcriptase following the manufactory protocol (Invitrogen). Gene specific PCR was performed using 10 μl of 2X HotStart Taq PCR Master Mix (Roche), 2.5 μM each of

the RT primer, used for cDNA synthesis, and a gene specific primer (niiA forward, 5′-CTGGTAGACTGACGAGGA-3′ or niaD forward, 5′-GACACCGGATAGAGAGAC-3′), 2 min at 95°C followed by 30 cycles of 30 s at 95°C, 30 s at 55°C and 60 s at 72°C with a final 10 min incubation at 72°C. PCR reaction products were purified after gel electrophoresis and cloned into pGEM-T Easy (Promega). Randomly selected clones were subject to Sanger sequencing (GATC).

Statistical analysis of quantitative northern data (Figures 1 and 2) was undertaken to determine if for any one strain there was a significant difference between histone transcript levels at t_0 and t_{20} for any one strain and if there was a significant difference between the regulatory response of any mutant strain and the WT. The regulatory response for each strain was calculated as the proportion of the normalized transcript level present at t_{20} compared to the level observed at t_0. The data were assumed to have a normal distribution. To determine if any two means were significantly different pairwise comparisons were made using either the two-tailed Student's *t*-test, when comparing two distributions with equal variances, or the two-tailed Welch's *t*-test, when comparing two distributions with unequal variances. The two distributions were considered to be significantly different if the *t*-test *p*-value was less than or equal to .05. To determine equal or unequal variance for each pairwise comparison the *F*-test was used (Snedecor and Cochran, 1989).

4.3 | CutA(109-460) and CutB(248-694) expression and purification

The *cutA*(109-460) coding region was amplified from *A. nidulans* cDNA by PCR (CutA_109_For 5′-AAGTTCTGTTTCAG GGCCCGATGTCTTTTTTCCGCAGAAGAATGCC-3′ and CutA_460_RevCompl 5′-TTGGCCACACCAGCCACCACCTTC-3′) and cloned using In-Fusion® HD Cloning Kit into the pOPINF vector (Addgene) yielding pOPINF-CutA(109-460). This plasmid was transformed into *E. coli* SoluBL21(DE3) and used for overexpression; the resulting stain was grown at 37°C in Terrific Broth supplemented with 100 μg/ml of ampicillin until reaching an OD_{600} between 0.6 and 0.8. The incubation temperature was then reduced to 18°C and protein production was induced by addition of 0.5 mM isopropyl β-D-1-thiogalactopyranoside (IPTG). After 18 h incubation cells were harvested with a 15 min centrifugation step at 3,000 *g* and resuspended in 20 mM Tris–HCl pH 8.5, 500 mM NaCl, 5 mM MgCl$_2$, 1 mM TCEP, supplemented with an ethylenediaminetetraacetic acid (EDTA)-free protease inhibitor cocktail (Roche), 2.5 μg/ml DNase I, 0.1% Triton X100. Cells were lysed at 4ªC (in an ice bath) using sonication (Sonics Inc.) consisting of five cycles of a 45 second pulse (60%) and a 1 min pause. Lysates were clarified with a 40 min centrifugation step at 40,000 *g* and filtered using a 0.22 μm filter prior to fast protein liquid chromatography (FPLC). Initial purification employed ion metal affinity chromatography (IMAC) in a 5 ml His-Trap HP column (GE healthcare), with the protein eluted using a step gradient of imidazole (20-300-500 mM). The sample was buffer exchanged into 20 mM

Tris–HCl pH 8.5, 200 mM NaCl, 5 mM MgCl$_2$, and 1 mM TCEP using Zeba 7K MWCO Desalting Columns (Thermo Scientific) and incubated overnight at 4°C with His$_6$ tagged 3C protease for tag removal. The cleaved protein was isolated by reverse IMAC in a 1 ml His-Trap HP column (GE healthcare). The cleaved protein was buffer exchanged into 20 mM Tris–HCl pH 8.5, 10 mM NaCl, and 1 mM TCEP using Zeba 7K MWCO Desalting Columns (Thermo Scientific) and further purified using ion exchange chromotography in a 5 ml HiTrap Q HP column (GE Healthcare) and the protein eluted using a linear gradient of NaCl (10–500 mM). CutA(109-460) was collected at a concentration of 25 mM NaCl and finally purified using a Superdex-200 10/300 gel filtration column (GE Healthcare) equilibrated in 15 mM Tris–HCl pH 8.5, 100 mM NaCl, and 1 mM TCEP.

The *cutB* (248-694) coding region was amplified from *A. nidulans* cDNA by PCR CutB_For248 (5′-AAGTTCTGTTTCAGGGCCC GACTCTACATCTGGGCACAAGGCTCC-3′ and CutB_Rev694_Compl 5′-ATGGTCTAGAAAGCTTTAGCTGACCGCGATGAGCCCTTTC-3′) and cloned using In-Fusion® HD Cloning Kit into pOPINF yielding pOPINF-CutB(248-694). Expression and purification were carried out as described for CutA except that after purification in the His-Trap HP column the protein was collected, the salt concentration adjusted to 50 mM for the nucleotide transferase activity and used immediately for analysis.

4.4 | Recombinant expression and purification of the catalytically inactive CutA(D214A), CutA(D216A) and CutB(D314A D316A) mutants

Using the template plasmids, pOPINF-CutA(109-460) and pOPINF-CutB(248-694), site-directed mutagenesis (QuikChange Site-Directed Mutagenesis kit, Stratagene) was used to generate the CutA(D214A), CutA(D216A), and CutB(D314A D316A) mutants using D101AFor 5′-CTAGCGACTCGGCGGTCGACATTTG-3′ and D101ARev_ Compl 5′-CAAATGTCGACCGCCGAGTCGCTAG-3′, D103AFor 5′-GACTCGGATGTCGCGATTTGTATAACT-3′ and D103ARev_Compl 5′-AGTTATACAAATCGCGACATCCGAGTC-3′) or cutBD312/4A_ For: 5′-CCAATGCCGcTATCGcTCTTGTCCTCCTCTCCAC-3′ and cutBD312/4ARev 5′-GACAAGAGCGATAGCGGCATTGGGAAGAT ACAGT-3′, respectively. This resulted in the construction of plasmids pOPINF-CutA(D214A), pOPINF-CutA(D216A), and CutB(D314A-D316A) which were validated by sequencing. Expression and purification of these mutant proteins were carried out as described above for the WT proteins. Protein purity was confirmed by SDS–PAGE (Figure S6) and concentrations were estimated using UV spectroscopy (A$_{280}$ nm).

4.5 | Nucleotide transferase activity

RNA oligonucleotides, labeled with Fluorescein (6-FAM) at the 5′ terminus, were purchased from Dharmacon. To assay the non-templated extension of the fluorescein labeled RNA oligonucleotide, reactions (generally 25 μl) were prepared in buffer containing 10 mM Tris–HCl pH 7.9, 50 mM NaCl, 10 mM MgCl$_2$ and 1 mM DTT. The reactions were programmed with protein, RNA substrates, and NTPs at the concentrations and in the combinations indicated in the figure legends. These reactions were incubated at 21°C for up to 80 min (see figure legends) and were subsequently stopped by adding an equal volume of 100 mM EDTA and 2% sodium dodecyl sulfate (SDS). Finally, products were denatured at 70°C and separated by gel electrophoresis in a 15% polyacrylamide/7 M urea gel. The gels were scanned and quantified using a Typhoon imager (GE Healthcare).

AUTHOR CONTRIBUTIONS

Experimental design and planning (MXC, IYM, OM, SRC, and PF), production and analysis of data (AMP, DP, N B-M, IB, SM, IYM, and MXC), preparation of the manuscript (IYM, SRC, and MXC).

ORCID

Mark X. Caddick https://orcid.org/0000-0002-5489-6557

REFERENCES

Caddick, M.X., Jones, M.G., van Tonder, J.M., le Cordier, H., Narendja, F., Strauss, J., et al. (2006) Opposing signals differentially regulate transcript stability in *Aspergillus nidulans*. *Molecular Microbiology*, 62, 509–519.

Celik, A., He, F. and Jacobson, A. (2017) NMD monitors translational fidelity 24/7. *Current Genetics*, 63, 1007–1010.

Chang, H., Lim, J., Ha, M. and Kim, V.N. (2014) TAIL-seq: genome-wide determination of poly(A) tail length and 3′ end modifications. *Molecular Cell*, 53, 1044–1052.

Cheng, Z.F. and Deutscher, M.P. (2005) An important role for RNase R in mRNA decay. *Molecular Cell*, 17, 313–318.

Choe, J., Ahn, S.H. and Kim, Y.K. (2014) The mRNP remodeling mediated by UPF1 promotes rapid degradation of replication-dependent histone mRNA. *Nucleic Acids Research*, 42, 9334–9349.

Clutterbuck, A.J. (1974) Aspergillus nidulans. In: King, R.C. (Ed.), *Handbook of Genetics, Vol. 1: Bacteria, Bacteriophage and Fungi.* 1 New York: Plenum Press. 447–510.

Clutterbuck, A.J. (1993) Aspergillus nidulans. In: O'Brian, S.J. (Ed.), *Genetic Maps, Vol. 3.* Locus Maps of Complex Genomes. 3 6, Cold Spring Harbor, NY: Cold Spring Harbor Laboratory Press. 3.71–3.84.

Cove, D.J. (1966) Induction and repression of nitrate reductase in fungus *Aspergillus nidulans*. *Biochimica et Biophysica Acta*, 113, 51–56.

Cui, J., Sartain, C.V., Pleiss, J.A. and Wolfner, M.F. (2013) Cytoplasmic polyadenylation is a major mRNA regulator during oogenesis and egg activation in Drosophila. *Developmental Biology*, 383, 121–131.

Elledge, S.J., Zhou, Z., Allen, J.B. and Navas, T.A. (1993) DNA damage and cell cycle regulation of ribonucleotide reductase. *BioEssays*, 15, 333–339.

Fernandez-Moya, S.M., Bauer, K.E. and Kiebler, M.A. (2014) Meet the players: local translation at the synapse. *Frontiers in Molecular Neuroscience*, 7, 84.

Graves, R.A. and Marzluff, W.F. (1984) Rapid reversible changes in the rate of histone gene transcription and histone mRNA levels in mouse myeloma cells. *Molecular and Cellular Biology*, 4, 351–357.

Hoefig, K.P., Rath, N., Heinz, G.A., Wolf, C., Dameris, J., Schepers, A., et al. (2013) Eri1 degrades the stem-loop of oligouridylated histone mRNAs to induce replication-dependent decay. *Nature Structural & Molecular Biology*, 20, U73–U97.

Kaygun, H. and Marzluff, W.F. (2005a) Regulated degradation of replication-dependent histone mRNAs requires both ATR and Upf1. *Nature Structural & Molecular Biology*, 12, 794–800.

Kaygun, H. and Marzluff, W.F. (2005b) Translation termination is involved in histone mRNA degradation when DNA replication is inhibited. *Molecular and Cellular Biology*, 25, 6879–6888.

Kobylecki, K., Kuchta, K., Dziembowski, A., Ginalski, K. and Tomecki, R. (2017) Biochemical and structural bioinformatics studies of fungal CutA nucleotidyltransferases explain their unusual specificity toward CTP and increased tendency for cytidine incorporation at the 3′-terminal positions of synthesized tails. *RNA*, 23, 1902–1926.

Koc, A., Wheeler, L.J., Mathews, C.K. and Merrill, G.F. (2004) Hydroxyurea arrests DNA replication by a mechanism that preserves basal dNTP pools. *Journal of Biological Chemistry*, 279, 223–230.

Kurosaki, T., Miyoshi, K., Myers, J.R. and Maquat, L.E. (2018) NMD-degradome sequencing reveals ribosome-bound intermediates with 3′-end non-templated nucleotides. *Nature Structural & Molecular Biology*, 25, 940–950.

Lacava, J., Houseley, J., Saveanu, C., Petfalski, E., Thompson, E., Jacquier, A., et al. (2005) RNA degradation by the exosome is promoted by a nuclear polyade nylation complex. *Cell*, 121, 713–724.

Lackey, P.E., Welch, J.D. and Marzluff, W.F. (2016) TUT7 catalyzes the uridylation of the 3′ end for rapid degradation of histone mRNA. *RNA*, 22, 1673–1688.

le Pen, J., Jiang, H., di Domenico, T., Kneuss, E., Kosalka, J., Leung, C., et al. (2018) Terminal uridylyltransferases target RNA viruses as part of the innate immune system. *Nature Structural & Molecular Biology*, 25, 778–786.

Maquat, L.E. (2002) Nonsense-mediated mRNA decay. *Current Biology*, 12, R196–R197.

Marzluff, W.F. and Koreski, K.P. (2017) Birth and death of histone mRNAs. *Trends in Genetics*, 33, 745–759.

Meaux, S.A., Holmquist, C.E. and Marzluff, W.F. (2018) Role of oligouridylation in normal metabolism and regulated degradation of mammalian histone mRNAs. *Philosophical Transactions of the Royal Society of London. Series B, Biological sciences*, 373, 20180170.

Mohanty, B.K. and Kushner, S.R. (2000) Polynucleotide phosphorylase, RNase II and RNase E play different roles in the in vivo modulation of polyadenylation in Escherichia coli. *Molecular Microbiology*, 36, 982–994.

Morozov, I.Y. and Caddick, M.X. (2012) Cytoplasmic mRNA 3′ tagging in eukaryotes: does it spell the end? *Biochemical Society Transactions*, 40, 810–814.

Morozov, I.Y., Jones, M.G., Gould, P.D., Crome, V., Wilson, J.B., Hall, A.J., et al. (2012) mRNA 3′ tagging is induced by nonsense-mediated decay and promotes ribosome dissociation. *Molecular and Cellular Biology*, 32, 2585–2595.

Morozov, I.Y., Jones, M.G., Razak, A.A., Rigden, D.J. and Caddick, M.X. (2010) CUCU modification of mRNA promotes decapping and transcript degradation in *Aspergillus nidulans*. *Molecular and Cellular Biology*, 30, 460–469.

Morozov, I.Y., Martinez, M.G., Jones, M.G. and Caddick, M.X. (2000) A defined sequence within the 3′ UTR of the areA transcript is sufficient to mediate nitrogen metabolite signalling via accelerated deadenylation. *Molecular Microbiology*, 37, 1248–1257.

Morozov, I.Y., Negrete-Urtasun, S., Tilburn, J., Jansen, C.A., Caddick, M.X., Arst, H.N., et al. (2006) Nonsense-mediated mRNA decay mutation in *Aspergillus nidulans*. *Eukaryotic Cell*, 5, 1838–1846.

Mullen, T.E. and Marzluff, W.F. (2008) Degradation of histone mRNA requires oligouridylation followed by decapping and simultaneous degradation of the mRNA both 5′ to 3′ and 3′ to 5′. *Genes & Development*, 22, 50–65.

Nachtergaele, S. and He, C. (2018) Chemical modifications in the life of an mRNA transcript & (Ed.) *Annual Review of Genetics*, Vol. 52, 349–372.

Norbury, C.J. (2013) Cytoplasmic RNA: a case of the tail wagging the dog. *Nature Reviews Molecular Cell Biology*, 14, 643–653.

Nousch, M., Minasaki, R. and Eckmann, C.R. (2017) Polyadenylation is the key aspect of GLD-2 function in *C. elegans*. *RNA*, 23, 1180–1187.

Nousch, M., Yeroslaviz, A., Habermann, B. and Eckmann, C.R. (2014) The cytoplasmic poly(A) polymerases GLD-2 and GLD-4 promote general gene expression via distinct mechanisms. *Nucleic Acids Research*, 42, 11622–11633.

Novotný, I., Podolská, K., Blažíková, M., Valášek, L.S., Svoboda, P. and Staněk, D. (2012) Nuclear LSm8 affects number of cytoplasmic processing bodies via controlling cellular distribution of Like-Sm proteins. *Molecular Biology of the Cell*, 23, 3776–3785.

Pan, K.W., Huang, Z., Lee, J.T.H. and Wong, C.M. (2015) Current perspectives on the role of TRAMP in nuclear RNA surveillance and quality control. *Research and Reports in Biochemistry*, 5, 111–117.

Platt, A., Langdon, T., Arst, H.N. Jr, Kirk, D., Tollervey, D., Sanchez, J.M. and et al(1996) Nitrogen metabolite signalling involves the C-terminus and the GATA domain of the *Aspergillus* transcription factor AREA and the 3′ untranslated region of its mRNA. *EMBO Journal*, 15, 2791–2801.

Radford, H.E., Meijer, H.A. and de Moor, C.H. (2008) Translational control by cytoplasmic polyadenylation in Xenopus oocytes. *Biochimica et Biophysica Acta-Gene Regulatory Mechanisms*, 1779, 217–229.

Rissland, O.S. and Norbury, C.J. (2009) Decapping is preceded by 3′ uridylation in a novel pathway of bulk mRNA turnover. *Nature Structural & Molecular Biology*, 16, 616–U56.

Sanicola, M., Ward, S., Childs, G. and Emmons, S.W. (1990) Identification of a Caenorhabditis elegans histone H1 gene family. Characterization of a family member containing an intron and encoding a poly(A)+ mRNA. *Journal of Molecular Biology*, 212, 259–68.

Slevin, M.K., Meaux, S., Welch, J.D., Bigler, R., de Marval, P.L.M., Su, W. et al(2014) Deep sequencing shows multiple oligouridylations are required for 3′ to 5′ degradation of histone mRNAs on polyribosomes. *Molecular Cell*, 53, 1020–1030.

Stagno, J., Aphasizheva, I., Rosengarth, A., Luecke, H. and Aphasizhev, R. (2007) UTP-bound and apo structures of a minimal RNA uridylyltransferase. *Journal of Molecular Biology*, 366, 882–899.

Snedecor, G.W. & Cochran, W.G. (1989) *Statistical Methods*. Eighth Edition, Iowa State University Press,

Subtelny, A.O., Eichhorn, S.W., Chen, G.R., Sive, H. and Bartel, D.P. (2014) Poly(A)-tail profiling reveals an embryonic switch in translational control. *Nature*, 508, 66–71.

Szewczyk, E., Nayak, T., Oakley, C.E., Edgerton, H., Xiong, Y., Taheri-Talesh, N., et al. (2006) Fusion PCR and gene targeting in *Aspergillus nidulans*. *Nat Protocols*, 1, 3111–3120.

Thomas, M.P., Liu, X., Whangbo, J., McCrossan, G., Sanborn, K.B., Basar, E., et al. (2015) Apoptosis triggers specific, rapid, and global mRNA decay with 3′ uridylated intermediates degraded by DIS3L2. *Cell Reports*, 11, 1079–89.

Vanacova, S., Wolf, J., Martin, G., Blank, D., Dettwiler, S., Friedlein, A., et al. (2005) A new yeast poly(A) polymerase complex involved in RNA quality control. *Plos Biology*, 3, 986–997.

Warkocki, Z., Liudkovska, V., Gewartowska, O., Mroczek, S. and Dziembowski, A. (2018) Terminal nucleotidyl transferases (TENTs) in mammalian RNA metabolism. *Philosophical Transactions of the Royal Society B-Biological Sciences*, 373.

Zigackova, D. and Vanacova, S. (2018) The role of 3′ end uridylation in RNA metabolism and cellular physiology. *Philosophical Transactions of the Royal Society B-Biological Sciences*, 373, 20180171.

Zuker, M. (2003) Mfold web server for nucleic acid folding and hybridization prediction. *Nucleic Acids Research*, 31, 3406–3415.

SUPPORTING INFORMATION

Additional Supporting Information may be found online in the Supporting Information section.